Molecular Engineering of Membrane Nanopores

Stefan Howorka

University College London, Institute of Structural and Molecular Biology, Department of Chemistry, London, UK

Membrane nanopores – hollow nanoscale barrels that puncture biological or synthetic membranes – have become powerful tools in chemical- and bio-sensing, and have achieved notable success in portable DNA sequencing. The pores can be self-assembled from a variety of materials, including proteins, peptides, synthetic-organic compounds, and, more recently, DNA. But which building material is best for which application, and what is the relationship between pore structure and function? In this Review, I critically compare the characteristics of the different building materials, and explore the influence of the building material on pore structure, dynamics and function. I also discuss the future challenges of developing nanopore technology, and explore what the next-generation of nanopore structures could be and where further practical applications might emerge.

Membrane nanopores are the most important border crossings in the molecular world. They form water-filled openings across membrane barriers composed of lipids or semifluid polymers in order to transport ionic or molecular cargo (Box 1). Given their small dimensions, nanopores function as size-selective filters that can limit transport to individual molecules. Nanopores can also select molecules based on charge and other physicochemical properties, and act as stimulus-responsive molecular valves that open or close and thereby regulate transport across membranes.

Reflecting these functions, membrane nanopores have been exploited for many applications. Pores can help sequence individual DNA strands[1-4], sense a wide range of analytes of biomedical and environmental relevance[5-11], and study single-molecule chemistry and biophysics. They can also regulate transport across cellular bilayers[12,13] or drug-delivery vesicles[14,15], or rupture membranes of bacterial pathogens[16]. Sensing and biophysical studies can also be realized with the related class of solid-state pores fabricated in thin non-organic films or materials[5,9,10,17-21]. These are, however, outside the main focus of this review.

In tune with the numerous applications, membrane nanopores can be composed of several different materials. Historically, protein and peptide pores were the first to be used given their pre-defined structure and ease of engineering. These biological pores later inspired the creation of artificial versions built from synthetic organic materials. The most recent nanopore class is obtained from folded DNA strands. As a characteristic, almost all pores can be formed in bottom-up fashion by simple self-assembly of the smaller building units. In this context, building material is used as loose term that encompasses the smallest unit (e.g. amino acids for proteins), secondary structure elements, and higher-order architectures.

With nanopore technology rapidly expanding, there are numerous unanswered fundamental questions about the construction and function of membrane pores, specifically about structure-function relationship. For example, what are the characteristics of the building materials, and how do they differ in terms of chemical tuneability, and suitability for bottom-up design? Furthermore, how do these characteristics influence the pores' structure, dynamics, function and applications? Answering these questions can contribute to a coherent understanding that underpins the rational design of advanced membrane nanopores. Knowing the strengths and weaknesses can also help select the most suitable building material for a given pore application. A survey of existing pores may finally identify future engineering targets. Excellent existing publications describe a single or two pore types but very few cover all[7-10,22-30].

This review compares the four membrane pore classes to obtain a comprehensive picture of all building materials and their impact on pore design, structure and function (Box 2). An overview first clarifies what constitutes a membrane nanopore and relates their advantages and disadvantages to solid-state pores. The subsequent four sections cover membrane pores composed of protein, peptide, DNA, and synthetic organic molecules, to identify similarities and differences. For each of these classes, prominent natural or engineered pores, strengths and weaknesses of the building material, and typical applications are described. The review concludes by highlighting sophisticated biological membrane proteins that can inspire the design of advanced nanopores.

Membrane nanopores vs. solid-state pores

A membrane pore is a hollow nanobarrel with a width usually in the range of 1-5 nm that punctures a biological or synthetic semifluid membrane[31,32]. The detailed barrel structure and transport properties have to be experimentally verified to establish whether a pore is present (see Box 3). Relying solely on transport assays without structural confirmation can be deceiving because synthetic lipids can locally deform the fluid bilayer[33] to yield pore-like electrical and optical read-out traces. However, high-resolution structural analysis is not possible for several peptide and synthetic pores that assemble exclusively in the membrane[24,26,34]. These are nevertheless covered here provided a membrane-spanning pore is strongly supported by its architecture and structural data. The exciting class of carrier ionophores is not discussed as they do not form a contiguous nanobarrel[35,36].

What are the advantages of membrane pores over solid-state pores within inorganic or polymeric films? By inserting into lipid bilayers, assembled pores are compatible with applications involving vesicles and cells[12,13] as well as membrane-based analysis platforms[1-4]. In addition, facile engineering with atomistic precision can tune the pores' dimensions, dynamics, and interactions with other molecules to a greater extent than classical solid-state materials such as silicon nitride or silicon dioxide.

The advantage of membrane pores on atomic precision is, however, increasingly rivalled by recent advances in solid-state pores formed inside atom-layer thin sheets of graphene[18] and MoS_2[20]. Pores in these synthetic materials are so small that they approach the size of individual nucleotides. The pores could therefore offer the necessary spatial resolution for nanopore DNA sequencing. As additional advantage, solid-state pores have great chemical stability and withstand buffer conditions incompatible with fluid membranes. One striking example is the use of MoS_2 pores with ionic liquids. These liquids are of high viscosity and slow down the nucleotide translocation through the pore so that the different isolated nucleotides can be resolved[20].

Solid-state nanopores are also of higher mechanical stability than lipid bilayers even though the latter's shortcoming can be addressed by several approaches[37]. These include the reduction of the lateral bilayer size[38] via droplet interface bilayers[39,40], the use of hydrogels or inorganic supports[41,42], the inclusion of polymerizable lipids[43,44], or the replacement of lipids with amphiphilic polymers[31,32]. Solid-state materials also make it easy to control how many pores are fabricated into the thin sheets[18,45-49]. Achieving one channel per membrane unit is essential for single-molecule DNA sequencing but challenging with membrane pores that stochastically insert into the semi-fluid membrane. As another advantage, solid-state pores can easily be read out with advanced physical tunneling methods not readily compatible with membrane nanopore systems[19]. Nevertheless, membrane nanopores offer greater chemical, structural and nanomechanical tuneability as detailed in the following chapters.

Protein pores

Given their multiple favorable features, protein pores are the current workhorses in nanopore-based DNA sequencing and single-molecule studies[1,5] due to a range of favorable features (Box 2). The protein pores of biological origin are of varied shape (examples listed below) and usually have atomistically defined and structurally stable scaffolds which facilitate rational engineering. Furthermore, proteins are made up of modular architectural units such as β-sheets and α-helices. Structural fine-tuning can be achieved with amino acids of different charges, size, functional groups, and hydrophobicity. As other advantage, proteins are produced in cells or cellular extracts from genetically engineered DNA templates. Consequently, it is easy to replace, add or delete amino acids at defined positions, or fuse functional protein domains[50]. Engineering can also help remove interfering floppy parts[51] or increase pore stability[52].

While benefiting from biology, engineering of protein pores can tap into the rich repertoire of synthetic chemistry to tailor the pores' structure and function (Box 2). Chemical interventions include the non-covalent placement of molecules into binding pockets, the covalent modification of selected natural amino acids[53], and the incorporation of non-natural amino acids[53]. Moreover, the polypeptide scaffold can be partially replaced with synthetic stretches via expressed protein ligation[54-56] where a biologically expressed protein fragment is fused to a synthetic peptide. Alternatively, a complete chemical synthesis can be achieved by native chemical ligation where two synthetic fragments are chemically fused[57].

Protein pores used in nanopore technology cover a broad range of shapes, and are usually oligomeric and constitutively open. Most are bacterial cytotoxins or conduits for passive transport. The protein pore used as reference is the cytotoxic heptameric αHL (α-hemolysin)[58]. Sequencing and stochastic sensing was pioneered with this pore given its easy insertion into membranes, the hour-long inserted state, the virtual absence of intrinsic stochastic structural switching, and the stable pore geometry amenable to protein engineering. αHL features a transmembrane β-barrel of less than 2 nm width and an extramembrane cap (Fig. 1a). In the context of sequencing, αHL has been replaced by shuttle pores MspA[59] and CsgG[60]. Cytotoxic ClyA[61] (Fig. 1a) of wider lumen can accommodate small folded proteins[52]. OmpG[62] (Fig. 1a) and OmpF[63] are unusual given their composition of solely of single polypeptide chains, while octameric Wza has membrane-spanning α-helices[64]. Nanopore technology also uses the aerolysin pore[65], the potassium channel KscA[66], mechanosensitive MscL[67], and an engineered membrane-inserting version of the bacteriophage phi29 DNA packaging motor[68]; but not cholesterol-dependent cytolysins or other membrane attack complexes[69] due to their variable number of subunits and unpredictable pore diameter. In the following, the versatility of pores is

illustrated by detailing their uses in sequencing, sensing, single-molecule chemistry and biophysics, and cell biology and nanobiotechnology.

The premier application of protein pores is DNA strand sequencing[1-4]. In nanopore sequencing, individual single-stranded DNA molecules translocate through a channel with an internal narrow constriction that serves as reading head (Fig. 1b). Simultaneously recording ionic current through a single channel reveals a step-wise read-out pattern that reflects the base sequence (Fig. 1b). Nanopore sequencing is label-free and reads very long DNA strands not accessible by competing techniques. It directly detects chemically altered bases of biomedical relevance such as methylated or hydroxymethylated cytosine[70]. The approach is miniaturizable to the size of a memory stick and hence portable[1]. Nanopore sequencing also highlights the benefit of a defined pore scaffold and tunable building blocks. Only a channel with no more than 1.5 nm width can permit the passage of a single DNA strands as opposed to multiple simultaneously translocating strands. Pores with suitable dimensions are αHL[58], MspA[2,3], and CsgG[60]. Furthermore, the reading head can be optimized to better distinguish DNA sequences, such as by altering the constriction's diameter, height, and hydrophobicity by amino acid replacements[2-4]. Recently, aerolysin has been shown to resolve individual short oligonucleotides that are 2 to 10 bases long[65] indicating that this pore might also be developed for sequencing.

Pores are also single-molecule sensors for non-DNA analytes[5,71]. They help uncover scientifically relevant static or dynamic heterogeneities not accessible by conventional ensemble methods. In one popular sensing mode –stochastic sensing[71]- separate analyte molecules bind to a defined recognition within the pore to give rise to characteristic current blockades (Fig. 1c) that differ from the constant current level of the non-bound pore. Binding sites can be generated via genetic engineering and, optionally, with chemical modification. One example is a histidine patch that recognizes metal cations within the αHL pure lumen[72]. Another is a docking site for hollow β-cyclodextrin rings[73,74] that in turn distinguish small organic drug molecules[73] as well as biomedically relevant stereoisomers[75].

In the second strategy of stochastic sensing, molecular receptors are covalently attached to individual amino acids. Cysteine is a preferred residue as it is easily genetically introduced, and specifically chemically modified at neutral pH and ambient temperature. Several molecular receptors were coupled to cysteine such as DNA oligonucleotides[76,77] and protein ligands[78,79]. In these cases, the number and attachment position of molecular receptors was carefully controlled to achieve a clear and strong current signal upon analyte binding. For example, a single short DNA oligonucleotide was placed inside the 3 nm-wide cap lumen of αHL to enable hybridization with complementary DNA strands[76]. For larger protein analytes, multiple recognition agents were positioned close at the channel entrance[77]. In more extensive genetic engineering, a fusion was generated between a molecular recognition unit – a G-protein coupled receptor- and a signal generator –a potassium channel; analyte binding triggered a conformational relay to open the channel and cause a current signal[50].

When protein channels are applied to probe single-molecule chemistry, it is similarly essential to control where and how many receptors are attached to the pore. Several different chemistries were successfully examined at the single-molecule level. Examples are the photo-chemical isomerization of diazo-dyes[80], the kinetic isotopic effects in a quinone reduction[81], and organo-arsene reactions that were resolved at unprecedented kinetic resolution[82]. Reversible bond formation along multiple cysteines created a random molecular walker[83].

Protein pores are also excellent tools to study the physico-chemistry of individual organic and biological polymers. In this type of analysis, single polymers translocate through or

temporarily reside in a narrow pore without the need for an engineered binding site. The approach can examine a wide range of biophysical aspects[5]. These studies are not discussed further as channel engineering usually[84] does not have a key enabling role.

For cell biology and nanobiotechnology, pores have been engineered into stimulus-responsive nanovalves to control membrane permeability. This is useful when examining how a cell responds to a locally and temporally defined flux of ions or molecules. For optical triggering of neuronal current, the Shaker K^+ channel was modified with a channel blocker via an azobenzene linker. The chromophore's wavelength-dependent cis-trans photo-isomerization moved the blocker to and from the pore entrance and altered the current[12]. A related light gate was installed in the glutamate receptor[13]. To make membranes permeable for larger cargo, the up 3 nm-wide MscL channel was furnished at key sites with multiple spiropyran chromophores that undergo reversible light-induced charge separation and cause pore opening and re-sealing[85]. This nanodevices may be applied e.g. for drug delivery. Thermal triggering was achieved by genetically placing in αHL a polypeptide that adopts different temperature-dependent conformations[86]. Similarly, voltage-sensitivity was programmed by genetically engineering 49 arginine residues into the pore's β-barrel; it collapsed at one but re-opened at the other potential[87]. Related amino acid replacements installed a strong ion filter into the OmpF pore[88] while expressed protein ligation fine-tuned the selective filter for K^+ in the KscA ion channel[54]. These engineered channels can be used to build synthetic ionic networks[87].

Despite many advantages, protein pores have shortcomings (Box 2). Proteins can be immunogenic which limits their use in therapy. In addition, it is a challenge to create protein pores with many non-natural amino acids; these can expand the pores' function. The experimental hurdle could be overcome with native chemical ligation which fuses small synthetic peptides to larger biogenic protein fragments[89]. It is furthermore difficult to make predictable and drastic structural changes such as varying the number of subunits, with some rare exceptions[90]. Designing *de novo* pores is even more strenuous. Hence, there is a shortage of pores wide enough to accommodate proteins or other marcomolecules for sensing or transport. The following three chapters show that limited chemical scope can be overcome with peptides and synthetic materials, while DNA offers considerable freedom in *de novo* design.

Peptide pores

Peptide pores are smaller than proteins and have usually no more than 50 amino acid. The short length is an advantage because it is easier to include residues other than the standard set of 20 proteinogenic L-amino acids (Box 2). For example, peptides with D-amino acid can be obtained via the nonribosomal biosynthesis[91]. Furthermore, peptides may be entirely built from synthetic amino acid via solid-phase synthesis[22,92]. As a consequence, chemically diverse peptide pores feature new scaffolds and functions.

Several biological examples illustrate the chemical and structural characteristics of peptide pores. Antibiotic gramicidins have a length of only 15 alternating L- and D-amino acids and assemble into a β-helix in which all residues point outward[93] (Fig. 2a); this is different to protein β-barrels where sequential residues alternate between inward and outward orientation. Due to its short length, one gramicidin helix only spans one membrane leaflet but two half-channels can transiently dimerise to form a membrane-puncturing channel[94] (Fig. 2a). By comparison, the 48 residue-long antibiotic polytheonamide B[95] completely transverses the membrane as a related β-helix. Another antibiotic peptide, alamethicin, is composed of standard L- as well as non-traditional 2-aminoisobutyric acid and folds into a α-helix[96]. Once inserted into a membrane, alameticin forms ion-selective channels of four

to twelve subunits[96-98] (Fig. 2b) Other antimicrobial peptides puncture the membrane, but via mechanisms that do not involve defined barrel-like pores[99].

Gramicidin has inspired the design of synthetic peptide channels. In particular, the alternating D-L sequence of gramicidin was mimicked by D,L-peptide rings that form stacks via hydrogen bond stabilization[92] (Fig. 2c). Following the biological lead, synthetic peptide peptide nanotubes[16,92] were evaluated as antibiotic agents. The peptide rings exhibited fast and broad bactericidal activity against Gram positive and negative bacteria. The action was most likely mediated by the permeabilization and rupturing of bacterial membranes. As an advantage, the synthesis of the agents is simple, and their low molecular weight can improve bioavailability[92]. The cyclic nature improved proteolytic stability compared to linear peptides, and the wide combinatorial sequence space may be exploited to counter antimicrobial resistance.

Synthetic gramicidin channels with the classical helical scaffold enabled label-free sensing of catalytic activity at the single-molecule level[22,100]. This required attaching different reactive chemical or biochemical moieties at the peptide's ambient-accessible C-terminus. For example, functional azide or chemical protecting groups helped track cyclo-addition and hydrolysis reactions[22], while enzymatic substrates were used for phosphatases or proteases[101], or the binding of carbonic anhydrase[102]. The peptides were not digested by the protease as the peptide structure is mostly inserted inside the membrane and protected from proteolysis. Ionic read-outs did not show simple on-off patterns due to the transient nature of gramicidin pores. Furthermore, it was not possible to assign ionic blockades unambiguously to channel blocking by analytes; the alternative was pore dissociation into half-channels[22]. To compensate for this potential drawback, peptides were attached to an organic scaffold[103](see chapter on synthetic pores). Alternatively, reversible half-pore association can be exploited to detect protein binding via impedance spectroscopy using supported bilayer membranes[100].

Alamethicin has also inspired artificial biomimetic versions but these synthetic α-helices tend to aggregate. An important step was hence to computationally design water-soluble bundles of five, six, or seven α-helices that enclose a central channel[104] (Fig. 2d). Membrane insertion was also engineered with a *de novo* four-helix bundle that, remarkably, transported Zn^{2+} but not Ca^{2+} [105]. The α-helices were held together by hydrophobic interaction of alanine and phenylalanine residues, while the ion-conducting path was lined by electron-rich glutamic acid and histidine residues. α-helices were also designed to sense pH and assemble within acidic lysosomal vesicles into pores and thereby release cargo into the cytoplasm[15]. These peptides may be used for cell-internal drug release.

Clearly, the advantages of peptide pores are their simple access via solid-phase synthesis, the wide chemical parameter space, and their ability to readily insert into membranes given their small size. However, it is difficult to build large or complex nanopore architectures from scratch (Box 2). This reflects the generic challenges to predict the folding of new polypeptides even though progress is underway[104,105]. Alternatively, pores can be easily made from scratch with DNA.

DNA nanopores

The very recently pioneered DNA pores[106-108] are architectures based on modularly interconnected duplexes that make rational engineering simple. In general, DNA allows *de novo* design of complex structures up to tens of nanometers[109-113] and thereby overcomes limitations of proteins and polypeptides (Box 2). Molecular reasons for this advantage include the larger size of nucleotides compared to amino acids, the predictable assembly

of DNA strands into duplexes via well-known Watson Crick base pairing which contrasts the more intricate folding of polypeptides, and the higher persistence length of duplexes. Consequently, dedicated design software[114] treats duplexes as cylinders that can be freely extended and linked together via Holiday junction cross-overs[109] to achieve parallel alignment in a hexagonal or square lattice. A given DNA strand hence threads through several DNA duplexes, and the corresponding DNA sequences are calculated by the software[114]. In addition to bundles of parallel duplexes, a much wider range of geometries is possible with curved duplexes[115,116] and polyhedral wireframes with tunable angles between straight duplex modules[117,118]. Independent of their structure, assembly is achieved simply by heating up and cooling down a mixture of DNA strands of preselected sequences. In the classical scaffold-and-staple approach, a long biogenic scaffold strand is folded with shorter synthetic staple oligonucleotides into the defined DNA structure[110]. It is also possible to use solely synthetic oligonucleotides as DNA bricks[119].

Existing DNA nanopores are mostly based on parallel-aligned DNA duplexes with optional curved elements[106]. The first two independently created[106,107] membrane DNA pores share a structural core of six hexagonally arranged DNA duplexes that enclose a central 2 nm-wide channel and puncture the bilayer[106,107] (Fig. 3ab). The design can be easily adapted for different pore heights[14,120,121] and thicker walls[106] (Fig. 3a). The number of duplexes in the central core can be reduced to four thereby yielding a 0.5 nm channel[122]. The principle of parallel aligned duplexes can also be extended to build larger DNA nanopores. A pore design with duplex in square lattice arrangement led to 6 nm-wide channel lumen (Fig. 3c)[123]. In an alternative design, a membrane-puncturing channel of 4 nm composed of squarely arranged duplexes was docked onto a horizontal nanoscale plate that sits on top of the structure[124]. This pore was also shown to translocate double stranded DNA.

To enable insertion into hydrophobic bilayers, DNA pores carry lipid anchors such as cholesterol[14,106,122] (Fig. 3ac), phorphyrin[120,125] or tocopherol[124] either on their membrane spanning outer pore wall[14,107,121] or positions that face the bilayer head-groups[106]. Alternatively, the DNA backbone can be chemically altered to remove negative charges in the phosphates[107,120] (Fig. 3b). Nevertheless, the strongly negatively charged nature renders pores more difficult to insert into planar membranes while insertion into curved membranes with inherent lipid defect structures is easier[106]. Lipid-anchored DNA pores have been pre-dated by non-membrane nanofunnels[126] and nanoplates with a built-in nanoscale hole[127]. And lipid anchoring is also exploited for rationally designing membrane-floating rafts composed of interconnected DNA duplexes that do not puncture the bilayer[128-132].

The ease of *de novo* design with DNA is illustrated by the fabrication of a synthetic version of a ligand-gated ion channel[14] (Fig. 3d). A DNA-based lid on top of the channel blocked the lumen. But a matching DNA ligand could hybridize to the lid and thereby remove it to open up the channel entrance. The channel also distinguished with high selectivity the transported small-molecule cargo carrying a positive instead of a negative charge. The DNA device may be used for controlled drug release[133], and the building of synthetic cell-like or logic ionic networks[87,134].

The design of future DNA pores should consider that they structurally fluctuate more than protein pores (Box 2) and have ionically leaky walls[135,136]. Both issues can be countered by thicker pore walls[106], while leakiness does not occur for larger cargo such as fluorophores[14] or proteins. Depending on the lipid anchor, the membrane-spanning DNA duplexes also reorganizes the lipid bilayer at the interface to the outer pore wall. For example, lipid headgroups can point to the DNA[137] and -in an extreme case- lead to a small water-filled gap bilayer and pore[138]. As another characteristic, DNA pores are negatively charged with a maximum density of 1 per nm^2. This appears to be high but is actually about five times lower than the theoretical maximum charge density of proteins[84]

because DNA duplexes are less compact than proteins. Nevertheless, negative charges in the DNA backbone can be removed by chemical modification[107] or by replacement with neutral peptide nucleic acids[139]. Similarly, the chemical diversity DNA can be expanded by synthetic chemistry[140] but there are limits due to the requirement to form duplexes.

Synthetic-organic channels

Synthetic molecules and polymers offer the widest chemical repertoire for building pores (Box 2). Examples of representative scaffolds are mentioned in the following paragraphs. The design freedom means, however, the lack of a generic architectural principle or software that aids uniform rational design, something which is readily available for DNA. It can also be challenging to build organic pores larger than a few nanometers and stay open for several hours in electrical recordings; carbon nanotubes are an exception. It is also difficult to obtain high-resolution structural data as many synthetic pores often adopt their final conformation only after membrane insertion. Hence, careful assignment of functional activity is important[141]. But many powerful synthetic structures have been generated within these boundaries.

The range of artificial channels[24,25,34,142] covers stacks of macrocycles[25], synthetic oligomeric β-barrels[103], organic analogues of the water-selective aquaporin[143], as well as carbon nanotubes[144] (Fig. 4). Other examples are circular oligoarenes[145] and oligomeric, channel-active structures thought to assemble from oligo-tetrahydrofurans[34], nucleobase dimers[146], and other amphilipic compounds[147].

To form vertical stacks of porous macrocycles, crown ethers with seven oxygens were attached to a scaffold such α-helical oligo-leucine[148] (Fig. 4a). The number and spacing of crown ethers was carefully selected to match the thickness of the membrane. The concept of interlinked macrocyles is open and can integrate ethers of variable size or replace oxygen of ethers with nitrogen. Furthermore, different linkers can be used such as linear alkane chains, ferrocences, crown-ethers, or octiphenyls chains[141,149].

The linear octiphenyl was also used as structural backbone in rigid-rod β-barrel pores which are among the best characterized synthetic channels[103] (Fig. 4b). In these architectures, octiphenyl serves as a vertical rod that carries eight L-amino acid pentapeptides. Four of these branched rods assemble via H-bond-mediated interdigitation of the peptides that place them parallel to the membrane plane. Similar to biological β-barrels, every other amino acid residue is hydrophobic and faces the lipid bilayer while the remaining hydrophilic amino acids point towards the channel lumen, thereby providing an opportunity to attach functional modules[11]. The hollow nature of the synthetic pore was confirmed by electrical recordings, and by threading a linear polymer chains into the lumen followed by probing with AFM the differential width of filled and empty pores[150].

The principle of rigid-rod β-barrels was expanded by replacing peptides with aromatic moieties (naphthalenediimide, NDI). The NDI groups did not interact via H-bonds but rather formed as aromatic structures π-π stacking interactions. Consequently, interdigitation of NDIs assembled four of the branched rods into a π-stack pore[151]. In a further development, a hybrid between β-barrels and π-stacks was created by attaching NDIs to the peptide branches of the octiphenyl-rod β-barrels[11]. Relieved from their structural role, NDI could interact with a wide range of electron-rich intercalators. This host-guest principle was exploited for sensing applications, as described further below[11].

The design flexibility of synthetic building blocks also led to a functional mimic[152] of biological aquaporin water channels (Fig. 4c). Related to the previous architectures, oligophenyl were derivatized with peptides. The oligophenyl scaffold was, however,

circular to define the membrane-embedded channel core. Each phenyl of the circular five-membered arene was additionally carrying two short phenylalanine peptides of alternating D-L-D isomer sequence. Hydrogen-bonding between the peptide backbones stabilized the tubular structure. These pillar[5]arenes were of similar osmotic water permeability as aquaporin and could be assembled into 2D arrays within membranes to achieve high collective permeability[143,152].

Unlike the previous channels, carbon nanotubes have a scaffold that is completely covalently linked by fused six-membered carbon rings[144]. The fabrication of single-walled carbon nanotubes of 1.5 nm diameter is well known[153], and sonication-assisted cutting can produce tubes shorter than 10 nm to approach the thickness of membranes. Recently, lipid-coated short tubes were inserted into bilayer membranes and live cell to form channels[144] (Fig. 4d). The tubes transport protons at high speed[154], but also water, small ions and DNA[144]. Their conductance and ion selectivity could be tuned by local channel charges[144]. A recent extension of pores with fused carbon rings has been the creation of helically folded polymer that carries membrane-interacting linear aliphatic chains[155] (Fig. 4e).

Chemical nanopores can be applied to sense organic molecules in complex matrixes thereby mimicking tongues that differentiate subtle variations in chemical analytes. The core of a sensing platform comprises rigid-rod β-barrels with aromatic NDI groups, and several intercalating agents[11]. The set-up was able to detect sucrose, lactose, lactate, acetate, citrate and glutamate in foodstuff samples. The sensing mechanism relied on the covalent reaction of the intercalating agents with the enzymatic break-down products of the analytes, followed by the intercalation of the newly formed bioconjugates between the NDI groups to block the rigid-rod barrel. Key in differentiating between the analytes was the use of various intercalators with different conjugation kinetics. The advantage of this strategy was the ability to sense a large number of analytes with a small number of pores. Related synthetic membrane scaffolds were also turned into artificial photosystems[156]. Furthermore, carbon nanotubes could be a biomimetic platform for developing cell interfaces, studying transport in biological channels, and creating stochastic sensors.

Conclusions

Membrane nanpores have received attention due the successful use in nanopore sequencing and their contribution to single-molecule studies. Looking into the future, which new pores may be constructed and which new developments will follow? What are the challenges of nanopore technology? And is there another pore application that can make the transition from specialist laboratory to the real world, as DNA sequencing has achieved?

Developing new pores will follow the understanding that each of the four building materials influences the corresponding nanopores' structural precision, size, and chemical diversity, as described in this review. Each material has unique strengths (Box 2). For example, proteins achieve unrivaled atomistic definition, while DNA is ideal for building larger *de novo* structures. By comparison, peptides and organic compounds excel in chemical variety. The upside is that the most suitable material can be chosen for a given application. Protein pores are hence leading in sensing. By comparison, a competitive advantage of peptide pores is in live-cell applications to e.g. kill bacteria or destabilize membranes for drug release.

But none of the materials is without shortcomings (Box 2). An alternative are hybrid pores that combine the strengths of two building blocks and thereby compensate at least part of their weaknesses. Adding a second component can impart new function as shown by

attaching analyte-binding polymers[79] or oligonucleotides[76,77] to αHL, or linking chemical groups to gramicidines[22]. Building architectures from two structurally equal components is more challenging but feasible. Routes are to fuse a synthetic peptide to a complementary protein fragment[54,56], or to interweave organic octiphenyl rods and peptides into rigid-rod β-barrels[103]. However, the scope of structural hybrids has only been tapped, and complete categories are missing such conjugates of DNA with proteins, organic molecules, or peptides. In these hybrid pores, DNA is expected to provide a coarse scaffold while the other components create the fine-grained structure. Synergy can furthermore be obtained by inserting atomistically defined protein pores or DNA nanofunnels into solid-state pores[126,157]. To exploit these in ionic current sensing, a tight electrical seal between inner and outer pores will have to be formed.

Inspiration for future pores also comes from biological templates. For example, pores that span two bilayers without leakage are valuable targets[158] for the creation of synthetic cell-like networks[87]. Another aim is to go beyond simple pore transport and couple it to simultaneous chemical transformation of the cargo. To this end, biocatalytic enzymes can be placed inside wide pores[52] but leakage transport of cargo without simultaneous catalysis has to be avoided. An alternative is to transplant the small active site of enzymes into a narrow channel. This has been achieved by engineering the catalytic triade of cysteine-histidine-glutamic acid inside a bundle of seven peptide α-helices[159]. Very high hydrolytic activity was obtained, but the water-soluble bundle was not yet engineered to insert into a membrane.

Other biological templates for re-engineering are membrane proteins that actively shuttle cargo across the membrane under expenditure of chemical energy. A direct synthetic replica is likely not possible due to the complex structure and multicomponent nature of biological templates such as the bacterial secretion systems for DNA or protein[160]. But functional aspects have been mimicked by transporting DNA using strand displacement[161] or ATP-driven DNA motor enzymes that can be membrane-associated[162] or membrane-embedded[68]. Similarly, pore-coupled unfoldases[163] can pull polypeptides through channels. Yet, it has not been possible to achieve active transport of smaller molecular cargo similar to nutrient and drugs-specific ABC transporters. This is unfortunate in light of the numerous potential applications in sensing, drug-delivery, and synthetic biology. Another biological template for bottom-up engineering is the F_OF_1 ATPase that produces rational movement by shuttling protons along a membrane gradient[164]. An additional inspiration is the β-barrel assembly machinery that helps fold membrane proteins by controlling when the threaded polypeptide is released from the machinery pore[165].

Is there another pore application that could make the transition from specialist laboratory to the real world? Clearly, the pore-based partial sequencing or mapping of unfolded proteins would have great prospect in diagnostics, agriculture, or homeland security. As an advantage, future reading of proteins could utilize the chip technology originally developed for DNA sequencing. Another likely trend will be the label-free sensing of other bioanalytes such as folded proteins. But what about real-world applications of pores outside sequencing and biosensing? One of the challenges in using pores as single-molecule sensors in biophysics and chemistry is the lack of standardization in read-out technology. Different pores are used for different applications because of the variety of analytes and scientific questions. In applications other than detection, challenges can also arise from the incomplete understanding of how pores insert into membranes. Furthermore, improvements in economically producing larger quantities of pores of consistent quality could help pave the way towards biomedical applications such as targeted cellular permeabilization or drug delivery. Addressing these topics will help use nanopores in more areas.

In conclusion, nanopore technology is a highly interdisciplinary research area that benefits from being at the interface between chemistry, biology and nanotechnology. Molecular engineering of membrane nanopores is an exciting activity, and designed nanopores have delivered impact in sequencing, single-molecule studies, and cell research. Exploiting the strengths of the different construction materials will lead to further developments and applications within technology and science.

REFERENCES

1. Quick, J. *et al.* Real-time, portable genome sequencing for Ebola surveillance. *Nature* **530,** 228-232 (2016).
2. Cherf, G. M. *et al.* Automated forward and reverse ratcheting of DNA in a nanopore at 5-Angstrom precision. *Nat. Biotechnol.* **30,** 344-348 (2012).
3. Manrao, E. A. *et al.* Reading DNA at single-nucleotide resolution with a mutant MspA nanopore and phi29 DNA polymerase. *Nat. Biotechnol.* **30,** 349-353 (2012).
4. Deamer, D., Akeson, M. & Branton, D. Three decades of nanopore sequencing. *Nat. Biotechnol.* **34,** 518-524 (2016).
5. Howorka, S. & Siwy, Z. Nanopore analytics: Sensing of single molecules. *Chem. Soc. Rev.* **38,** 2360-2384 (2009).
6. Wang, G., Wang, L., Han, Y., Zhou, S. & Guan, X. Nanopore stochastic detection: Diversity, sensitivity, and beyond. *Acc. Chem. Res.* **46,** 2867-2877 (2013).
7. Stoloff, D. H. & Wanunu, M. Recent trends in nanopores for biotechnology. *Curr. Opin. Biotechnol.* **24,** 699-704 (2013).
8. Reiner, J. E. *et al.* Disease detection and management via single nanopore-based sensors. *Chem. Rev.* **112,** 6431-6451 (2012).
9. Miles, B. N. *et al.* Single molecule sensing with solid-state nanopores: Novel materials, methods, and applications. *Chem. Soc. Rev.* **42,** 15-28 (2013).
10. Venkatesan, B. M. & Bashir, R. Nanopore sensors for nucleic acid analysis. *Nat. Nanotechnol.* **6,** 615-624 (2011).
11. Litvinchuk, S. *et al.* Synthetic pores with reactive signal amplifiers as artificial tongues. *Nat. Mater.* **6,** 576-580 (2007).
12. Banghart, M., Borges, K., Isacoff, E., Trauner, D. & Kramer, R. H. Light-activated ion channels for remote control of neuronal firing. *Nat. Neurosci.* **7,** 1381-1386 (2004).
13. Volgraf, M. *et al.* Allosteric control of an ionotropic glutamate receptor with an optical switch. *Nat. Chem. Biol.* **2,** 47-52 (2006).
14. Burns, J. R., Seifert, A., Fertig, N. & Howorka, S. A biomimetic DNA-based channel for the ligand-controlled transport of charged molecular cargo across a biological membrane. *Nat. Nanotechnol.* **11,** 152-156 (2016).
15. Zhang, Y. *et al.* Computational design and experimental characterization of peptides intended for ph-dependent membrane insertion and pore formation. *ACS Chem. Biol.* **10,** 1082-1093 (2015).
16. Fernandez-Lopez, S. *et al.* Antibacterial agents based on the cyclic D,L-alpha-peptide architecture. *Nature* **412,** 452-455 (2001).
17. Dekker, C. Solid-state nanopores. *Nat. Nanotechnol.* **2,** 209-215 (2007).
18. Heerema, S. J. & Dekker, C. Graphene nanodevices for DNA sequencing. *Nat. Nanotechnol.* **11,** 127-136 (2016).
19. Lindsay, S. The promises and challenges of solid-state sequencing. *Nat. Nanotechnol.* **11,** 109-111 (2016).
20. Feng, J. *et al.* Identification of single nucleotides in MoS_2 nanopores. *Nat. Nanotechnol.* **10,** 1070-1076 (2015).

21. Bell, N. A. & Keyser, U. F. Digitally encoded DNA nanostructures for multiplexed, single-molecule protein sensing with nanopores. *Nat. Nanotechnol.* **11,** 645-651 (2016).

22. Mayer, M. & Yang, J. Engineered ion channels as emerging tools for chemical biology. *Acc. Chem. Res.* **46,** 2998-3008 (2013).

23. Langecker, M., Arnaut, V., List, J. & Simmel, F. C. DNA nanostructures interacting with lipid bilayer membranes. *Acc. Chem. Res.* **47,** 1807-1815 (2014).

24. Fyles, T. M. Synthetic ion channels in bilayer membranes. *Chem. Soc. Rev.* **36,** 335-347 (2007).

25. Gokel, G. W. & Negin, S. Synthetic ion channels: From pores to biological applications. *Acc. Chem. Res.* **46,** 2824-2833 (2013).

26. Sakai, N. & Matile, S. Synthetic ion channels. *Langmuir* **29,** 9031-9040 (2013).

27. Bell, N. A. & Keyser, U. F. Nanopores formed by DNA origami: A review. *FEBS Lett.* **588,** 3564-3570 (2014).

28. Shi, W., Friedman, A. K. & Baker, L. A. Nanopore sensing. *Anal. Chem.* **89,** 157-188 (2017).

29. Majd, S. *et al.* Applications of biological pores in nanomedicine, sensing, and nanoelectronics. *Curr. Opin. Biotechnol.* **21,** 439-476 (2010).

30. Ayub, M. & Bayley, H. Engineered transmembrane pores. *Curr. Opin. Chem. Biol.* **34,** 117-126 (2016).

31. Meier, W., Nardin, C. & Winterhalter, M. Reconstitution of channel proteins in (polymerized) aba triblock copolymer membranes. *Angew. Chem. Int. Ed.* **39,** 4599-4602 (2000).

32. Nardin, C., Winterhalter, M. & Meier, W. Giant free-standing aba triblock copolymer membranes. *Langmuir* **16,** 7708–7712 (2010).

33. Mosgaard, L. D. & Heimburg, T. Lipid ion channels and the role of proteins. *Acc. Chem. Res.* **46,** 2966-2976 (2013).

34. Reiss, P. & Koert, U. Ion-channels: Goals for function-oriented synthesis. *Acc. Chem. Res.* **46,** 2773-2780 (2013).

35. De Riccardis, F., Izzo, I., Montesarchio, D. & Tecilla, P. Ion transport through lipid bilayers by synthetic ionophores: Modulation of activity and selectivity. *Acc. Chem. Res.* **46,** 2781-2790 (2013).

36. Li, H. *et al.* Efficient, non-toxic anion transport by synthetic carriers in cells and epithelia. *Nat. Chem.* **8,** 24-32 (2016).

37. Schmidt, J. Membrane platforms for biological nanopore sensing and sequencing. *Curr. Opin. Biotechnol.* **39,** 17-27 (2016).

38. Urban, M. *et al.* Highly parallel transport recordings on a membrane-on-nanopore chip at single molecule resolution. *Nano Lett.* **14,** 1674-1680 (2014).

39. Funakoshi, K., Suzuki, H. & Takeuchi, S. Lipid bilayer formation by contacting monolayers in a microfluidic device for membrane protein analysis. *Anal. Chem.* **78,** 8169-8174 (2006).

40. Holden, M. A., Needham, D. & Bayley, H. Functional bionetworks from nanoliter water droplets. *J. Am. Chem. Soc.* **129,** 8650-8655 (2007).

41. Jeon, T. J., Malmstadt, N. & Schmidt, J. J. Hydrogel-encapsulated lipid membranes. *J. Am. Chem. Soc.* **128,** 42-43 (2006).

42. Shim, J. W. & Gu, L. Q. Stochastic sensing on a modular chip containing a single-ion channel. *Anal. Chem.* **79,** 2207-2213 (2007).

43. Daly, S. M., Heffernan, L. A., Barger, W. R. & Shenoy, D. K. Photopolymerization of mixed monolayers and black lipid membranes containing gramicidin A and diacetylenic phospholipids. *Langmuir* **22,** 1215-1222 (2006).

44. Heitz, B. A., Jones, I. W., Hall, H. K., Jr., Aspinwall, C. A. & Saavedra, S. S. Fractional polymerization of a suspended planar bilayer creates a fluid, highly

stable membrane for ion channel recordings. *J. Am. Chem. Soc.* **132,** 7086-7093 (2010).

45. Wei, R. S., Gatterdam, V., Wieneke, R., Tampe, R. & Rant, U. Stochastic sensing of proteins with receptor-modified solid-state nanopores. *Nat. Nanotechnol.* **7,** 257-263 (2012).

46. Wang, Y., Zheng, D., Tan, Q., Wang, M. X. & Gu, L. Q. Nanopore-based detection of circulating microRNAs in lung cancer patients. *Nat. Nanotechnol.* **6,** 668-674 (2011).

47. Traversi, F. *et al.* Detecting the translocation of DNA through a nanopore using graphene nanoribbons. *Nat. Nanotechnol.* **8,** 939-945 (2013).

48. Wanunu, M. *et al.* Rapid electronic detection of probe-specific microRNAs using thin nanopore sensors. *Nat. Nanotechnol.* **5,** 807-814 (2010).

49. Yusko, E. C. *et al.* Controlling protein translocation through nanopores with bio-inspired fluid walls. *Nat. Nanotechnol.* **6,** 253-260 (2011).

50. Moreau, C. J., Dupuis, J. P., Revilloud, J., Arumugam, K. & Vivaudou, M. Coupling ion channels to receptors for biomolecule sensing. *Nat. Nanotechnol.* **3,** 620-625 (2008).

51. Chen, M., Khalid, S., Sansom, M. S. & Bayley, H. Outer membrane protein G: Engineering a quiet pore for biosensing. *Proc. Natl. Acad. Sci. U S A* **105,** 6272-6277 (2008).

52. Soskine, M. *et al.* An engineered ClyA nanopore detects folded target proteins by selective external association and pore entry. *Nano Lett.* **12,** 4895-4900 (2012).

53. Spicer, C. D. & Davis, B. G. Selective chemical protein modification. *Nat. Commun.* **5,** 4740 (2014).

54. Valiyaveetil, F. I., Leonetti, M., Muir, T. W. & MacKinnon, R. Ion selectivity in a semisynthetic K^+ channel locked in the conductive conformation. *Science* **314,** 1004-1007 (2006).

55. Focke, P. J. & Valiyaveetil, F. I. Studies of ion channels using expressed protein ligation. *Curr. Opin. Chem. Biol.* **14,** 797-802 (2010).

56. Lee, J. & Bayley, H. Semisynthetic protein nanoreactor for single-molecule chemistry. *Proc. Natl. Acad. Sci. U S A* **112,** 13768-13773 (2015).

57. Clayton, D. *et al.* Total chemical synthesis and electrophysiological characterization of mechanosensitive channels from *Escherichia coli* and *Mycobacterium tuberculosis*. *Proc. Natl. Acad. Sci. U S A* **101,** 4764-4769 (2004).

58. Song, L. *et al.* Structure of staphylococcal alpha-hemolysin, a heptameric transmembrane pore. *Science* **274,** 1859-1866 (1996).

59. Faller, M., Niederweis, M. & Schulz, G. E. The structure of a mycobacterial outer-membrane channel. *Science* **303,** 1189-1192 (2004).

60. Goyal, P. *et al.* Structural and mechanistic insights into the bacterial amyloid secretion channel CsgG. *Nature* **516,** 250-253 (2014).

61. Mueller, M., Grauschopf, U., Maier, T., Glockshuber, R. & Ban, N. The structure of a cytolytic alpha-helical toxin pore reveals its assembly mechanism. *Nature* **459,** 726-730 (2009).

62. Liang, B. & Tamm, L. K. Structure of outer membrane protein G by solution NMR spectroscopy. *Proc. Natl. Acad. Sci. U S A* **104,** 16140-16145 (2007).

63. Cowan, S. W. *et al.* Crystal structures explain functional properties of two *E. coli* porins. *Nature* **358,** 727-733 (1992).

64. Dong, C. *et al.* Wza the translocon for *E. coli* capsular polysaccharides defines a new class of membrane protein. *Nature* **444,** 226-229 (2006).

65. Cao, C. *et al.* Discrimination of oligonucleotides of different lengths with a wild-type aerolysin nanopore. *Nat. Nanotechnol.* **11,** 713-718 (2016).

66.   Doyle, D. A. *et al.* The structure of the potassium channel: Molecular basis of K$^+$ conduction and selectivity. *Science* **280,** 69-77 (1998).

67.   Chang, G., Spencer, R. H., Lee, A. T., Barclay, M. T. & Rees, D. C. Structure of the MscL homolog from *Mycobacterium tuberculosis*: A gated mechanosensitive ion channel. *Science* **282,** 2220-2226 (1998).

68.   Haque, F., Geng, J., Montemagno, C. & Guo, P. Incorporation of a viral DNA-packaging motor channel in lipid bilayers for real-time, single-molecule sensing of chemicals and double-stranded DNA. *Nat. Protoc.* **8,** 373-392 (2013).

69.   Dunstone, M. A. & Tweten, R. K. Packing a punch: The mechanism of pore formation by cholesterol dependent cytolysins and membrane attack complex/perforin-like proteins. *Curr. Opin. Struct. Biol.* **22,** 342-349 (2012).

70.   Laszlo, A. H. *et al.* Detection and mapping of 5-methylcytosine and 5-hydroxymethylcytosine with nanopore mspa. *Proc. Natl. Acad. Sci. U S A* **110,** 18904-18909 (2013).

71.   Bayley, H. & Cremer, P. S. Stochastic sensors inspired by biology. *Nature* **413,** 226-230 (2001).

72.   Braha, O. *et al.* Designed protein pores as components for biosensors. *Chem. Biol.* **4,** 497-505 (1997).

73.   Gu, L. Q., Braha, O., Conlan, S., Cheley, S. & Bayley, H. Stochastic sensing of organic analytes by a pore-forming protein containing a molecular adapter. *Nature* **398,** 686-690 (1999).

74.   Gu, L. Q., Cheley, S. & Bayley, H. Capture of a single molecule in a nanocavity. *Science* **291,** 636-640. (2001).

75.   Kang, X. F., Cheley, S., Guan, X. & Bayley, H. Stochastic detection of enantiomers. *J. Am. Chem. Soc.* **128,** 10684-10685 (2006).

76.   Howorka, S., Cheley, S. & Bayley, H. Sequence-specific detection of individual DNA-strands using engineered nanopores. *Nat. Biotechnol.* **19,** 636-639 (2001).

77.   Rotem, D., Jayasinghe, L., Salichou, M. & Bayley, H. Protein detection by nanopores equipped with aptamers. *J. Am. Chem. Soc.* **134,** 2781-2787 (2012).

78.   Howorka, S. *et al.* A protein pore with a single polymer chain tethered within the lumen. *J. Am. Chem. Soc.* **122,** 2411-2416 (2000).

79.   Movileanu, L., Howorka, S., Braha, O. & Bayley, H. Detecting protein analytes that modulate transmembrane movement of a polymer chain within a single protein pore. *Nat. Biotechnol.* **18,** 1091-1095 (2000).

80.   Loudwig, S. & Bayley, H. Photoisomerization of an individual azobenzene molecule in water: An on-off switch triggered by light at a fixed wavelength. *J. Am. Chem. Soc.* **128,** 12404-12405 (2006).

81.   Lu, S., Li, W. W., Rotem, D., Mikhailova, E. & Bayley, H. A primary hydrogen-deuterium isotope effect observed at the single-molecule level. *Nat. Chem.* **2,** 921-928 (2010).

82.   Shin, S. H., Steffensen, M. B., Claridge, T. D. & Bayley, H. Formation of a chiral center and pyrimidal inversion at the single-molecule level. *Angew. Chem. Int. Ed.* **46,** 7412-7416 (2007).

83.   Pulcu, G. S., Mikhailova, E., Choi, L. S. & Bayley, H. Continuous observation of the stochastic motion of an individual small-molecule walker. *Nat. Nanotechnol.* **10,** 76-83 (2015).

84.   Maglia, G., Restrepo, M. R., Mikhailova, E. & Bayley, H. Enhanced translocation of single DNA molecules through alpha-hemolysin nanopores by manipulation of internal charge. *Proc. Natl. Acad. Sci. U S A* **105,** 19720-19725 (2008).

85.   Kocer, A., Walko, M., Meijberg, W. & Feringa, B. L. A light-actuated nanovalve derived from a channel protein. *Science* **309,** 755-758 (2005).

86. Jung, Y., Bayley, H. & Movileanu, L. Temperature-responsive protein pores. *J. Am. Chem. Soc.* **128,** 15332-15340 (2006).

87. Maglia, G. *et al.* Droplet networks with incorporated protein diodes show collective properties. *Nat. Nanotechnol.* **4,** 437-440 (2009).

88. Miedema, H. *et al.* A biological porin engineered into a molecular, nanofluidic diode. *Nano Lett.* **7,** 2886-2891 (2007).

89. Bondalapati, S., Jbara, M. & Brik, A. Expanding the chemical toolbox for the synthesis of large and uniquely modified proteins. *Nat. Chem.* **8,** 407-418 (2016).

90. Stoddart, D. *et al.* Functional truncated membrane pores. *Proc. Natl. Acad. Sci. U S A* **111,** 2425-2430 (2014).

91. Reimer, J. M., Aloise, M. N., Harrison, P. M. & Schmeing, T. M. Synthetic cycle of the initiation module of a formylating nonribosomal peptide synthetase. *Nature* **529,** 239-242 (2016).

92. Montenegro, J., Ghadiri, M. R. & Granja, J. R. Ion channel models based on self-assembling cyclic peptide nanotubes. *Acc. Chem. Res.* **46,** 2955-2965 (2013).

93. Ketchem, R. R., Hu, W. & Cross, T. A. High-resolution conformation of gramicidin a in a lipid bilayer by solid-state NMR. *Science* **261,** 1457-1460 (1993).

94. Cifu, A. S., Koeppe, R. E., 2nd & Andersen, O. S. On the supramolecular organization of gramicidin channels. The elementary conducting unit is a dimer. *Biophys. J.* **61,** 189-203 (1992).

95. Inoue, M. *et al.* Total synthesis of the large non-ribosomal peptide polytheonamide b. *Nat. Chem.* **2,** 280-285 (2010).

96. Leitgeb, B., Szekeres, A., Manczinger, L., Vagvolgyi, C. & Kredics, L. The history of alamethicin: A review of the most extensively studied peptaibol. *Chem. Biodivers.* **4,** 1027-1051 (2007).

97. Pieta, P., Mirza, J. & Lipkowski, J. Direct visualization of the alamethicin pore formed in a planar phospholipid matrix. *Proc. Natl. Acad. Sci. U S A* **109,** 21223-21227 (2012).

98. Mayer, M., Kriebel, J. K., Tosteson, M. T. & Whitesides, G. M. Microfabricated teflon membranes for low-noise recordings of ion channels in planar lipid bilayers. *Biophys. J.* **85,** 2684-2695 (2003).

99. Fjell, C. D., Hiss, J. A., Hancock, R. E. & Schneider, G. Designing antimicrobial peptides: Form follows function. *Nat. Rev. Drug. Discov.* **11,** 37-51 (2012).

100. Cornell, B. A. *et al.* A biosensor that uses ion-channel switches. *Nature* **387,** 580-583 (1997).

101. Macrae, M. X. *et al.* A semi-synthetic ion channel platform for detection of phosphatase and protease activity. *ACS Nano* **3,** 3567-3580 (2009).

102. Mayer, M., Semetey, V., Gitlin, I., Yang, J. & Whitesides, G. M. Using ion channel-forming peptides to quantify protein-ligand interactions. *J. Am. Chem. Soc.* **130,** 1453-1465 (2008).

103. Sakai, N., Mareda, J. & Matile, S. Artificial beta-barrels. *Acc. Chem. Res.* **41,** 1354-1365 (2008).

104. Thomson, A. R. *et al.* Computational design of water-soluble alpha-helical barrels. *Science* **346,** 485-488 (2014).

105. Joh, N. H. *et al.* De novo design of a transmembrane $Zn2^+$-transporting four-helix bundle. *Science* **346,** 1520-1524 (2014).

106. Langecker, M. *et al.* Synthetic lipid membrane channels formed by designed DNA nanostructures. *Science* **338,** 932-936 (2012).

107. Burns, J., Stulz, E. & Howorka, S. Self-assembled DNA nanopores that span lipid bilayers. *Nano Lett.* **13,** 2351-2356 (2013).

108. Howorka, S. Nanotechnology. Changing of the guard. *Science* **352,** 890-891 (2016).

109. Seeman, N. C. Nanomaterials based on DNA. *Annu. Rev. Biochem.* **79,** 65-87 (2010).
110. Rothemund, P. W. Folding DNA to create nanoscale shapes and patterns. *Nature* **440,** 297-302 (2006).
111. Chen, Y. J., Groves, B., Muscat, R. A. & Seelig, G. DNA nanotechnology from the test tube to the cell. *Nat. Nanotechnol.* **10,** 748-760 (2015).
112. Pinheiro, A. V., Han, D., Shih, W. M. & Yan, H. Challenges and opportunities for structural DNA nanotechnology. *Nat. Nanotechnol.* **6,** 763-772 (2011).
113. Jones, M. R., Seeman, N. C. & Mirkin, C. A. Nanomaterials. Programmable materials and the nature of the DNA bond. *Science* **347,** 1260901 (2015).
114. Douglas, S. M. *et al.* Rapid prototyping of 3D DNA-origami shapes with caDNAno. *Nucleic Acids Res.* **37,** 5001-5006 (2009).
115. Dietz, H., Douglas, S. M. & Shih, W. M. Folding DNA into twisted and curved nanoscale shapes. *Science* **325,** 725-730 (2009).
116. Han, D. *et al.* DNA origami with complex curvatures in three-dimensional space. *Science* **332,** 342-346 (2011).
117. Zhang, F. *et al.* Complex wireframe DNA origami nanostructures with multi-arm junction vertices. *Nat. Nanotechnol.* **10,** 779-784 (2015).
118. Benson, E. *et al.* DNA rendering of polyhedral meshes at the nanoscale. *Nature* **523,** 441-444 (2015).
119. Ke, Y., Ong, L. L., Shih, W. M. & Yin, P. Three-dimensional structures self-assembled from DNA bricks. *Science* **338,** 1177-1183 (2012).
120. Burns, J. R., Al-Juffali, N., Janes, S. M. & Howorka, S. Membrane-spanning DNA nanopores with cytotoxic effect. *Angew. Chem. Int. Ed.* **53,** 12466-12470 (2014).
121. Burns, J. R. *et al.* Lipid bilayer-spanning DNA nanopores with a bifunctional porphyrin anchor. *Angew. Chem. Int. Ed.* **52,** 12069–12072 (2013).
122. Gopfrich, K. *et al.* DNA-tile structures induce ionic currents through lipid membranes. *Nano Lett.* **15,** 3134-3138 (2015).
123. Gopfrich, K. *et al.* Large-conductance transmembrane porin made from DNA origami. *ACS Nano* **10,** 8207-8214 (2016).
124. Krishnan, S. *et al.* Molecular transport through large-diameter DNA nanopores. *Nat. Commun.* **7,** 12787 (2016).
125. Seifert, A. *et al.* Bilayer-spanning DNA nanopores with voltage-switching between open and closed state. *ACS Nano* **9,** 1117-1126 (2015).
126. Bell, N. A. *et al.* DNA origami nanopores. *Nano Lett.* **12,** 512-517 (2012).
127. Wei, R., Martin, T. G., Rant, U. & Dietz, H. DNA origami gatekeepers for solid-state nanopores. *Angew. Chem. Int. Ed.* **51,** 4864-4867 (2012).
128. Czogalla, A. *et al.* Amphipathic DNA origami nanoparticles to scaffold and deform lipid membrane vesicles. *Angew. Chem. Int. Ed.* **54,** 6501-6505 (2015).
129. Kocabey, S. *et al.* Membrane-assisted growth of DNA origami nanostructure arrays. *ACS Nano* **9,** 3530-3539 (2015).
130. Johnson-Buck, A., Jiang, S., Yan, H. & Walter, N. G. DNA-cholesterol barges as programmable membrane-exploring agents. *ACS Nano* **8,** 5641-5649 (2014).
131. Yang, Y. *et al.* Self-assembly of size-controlled liposomes on DNA nanotemplates. *Nat. Chem.* **8,** 476-483 (2016).
132. Perrault, S. D. & Shih, W. M. Virus-inspired membrane encapsulation of DNA nanostructures to achieve in vivo stability. *ACS Nano* **8,** 5132-5140 (2014).
133. Mura, S., Nicolas, J. & Couvreur, P. Stimuli-responsive nanocarriers for drug delivery. *Nat. Mater.* **12,** 991-1003 (2013).
134. Villar, G., Graham, A. D. & Bayley, H. A tissue-like printed material. *Science* **340,** 48-52 (2013).

135. Maingi, V., Lelimousin, M., Howorka, S. & Sansom, M. S. Gating-like motions and wall porosity in a DNA nanopore scaffold revealed by molecular simulations. *ACS Nano* **9,** 11209-11217 (2015).

136. Yoo, J. & Aksimentiev, A. Molecular dynamics of membrane-spanning DNA channels: Conductance mechanism, electro-osmotic transport, and mechanical gating. *J. Phys. Chem. Lett.* **6,** 4680-4687 (2015).

137. Maingi, V. *et al.* Stability and dynamics of membrane-spanning DNA nanopores. *Nat. Commun.* **8,** 14784 (2017).

138. Gopfrich, K. *et al.* Ion channels made from a single membrane-spanning DNA duplex. *Nano Lett.* **16,** 4665-4669 (2016).

139. Ackermann, D. & Famulok, M. Pseudo-complementary pna actuators as reversible switches in dynamic DNA nanotechnology. *Nucleic Acids Res.* **41,** 4729-4739 (2013).

140. Edwardson, T. G., Carneiro, K. M., McLaughlin, C. K., Serpell, C. J. & Sleiman, H. F. Site-specific positioning of dendritic alkyl chains on DNA cages enables their geometry-dependent self-assembly. *Nat. Chem.* **5,** 868-875 (2013).

141. Chui, J. K. & Fyles, T. M. Ionic conductance of synthetic channels: Analysis, lessons, and recommendations. *Chem. Soc. Rev.* **41,** 148-175 (2012).

142. Sakaki, Y., Mareda, J. & Matile, S. Ion channels and pores, made from scratch. *Mol. Biosys.* **3,** 658-666 (2007).

143. Barboiu, M. & Gilles, A. From natural to bioassisted and biomimetic artificial water channel systems. *Acc. Chem. Res.* **46,** 2814-2823 (2013).

144. Geng, J. *et al.* Stochastic transport through carbon nanotubes in lipid bilayers and live cell membranes. *Nature* **514,** 612-615 (2014).

145. Negin, S., Daschbach, M. M., Kulikov, O. V., Rath, N. & Gokel, G. W. Pore formation in phospholipid bilayers by branched-chain pyrogallol[4]arenes. *J. Am. Chem. Soc.* **133,** 3234-3237 (2011).

146. Das, R. N., Kumar, Y. P., Schutte, O. M., Steinem, C. & Dash, J. A DNA-inspired synthetic ion channel based on g-c base pairing. *J. Am. Chem. Soc.* **137,** 34-37 (2015).

147. Fyles, T. M. How do amphiphiles form ion-conducting channels in membranes? Lessons from linear oligoesters. *Acc. Chem. Res.* **46,** 2847-2855 (2013).

148. Meillon, J. C. & Voyer, N. A synthetic transmembrane channel active in lipid bilayers. *Angew. Chem. Int. Ed.* **36,** 967-969 (1997).

149. Gilles, A. & Barboiu, M. Highly selective artificial K^+ channels: An example of selectivity-induced transmembrane potential. *J. Am. Chem. Soc.* **138,** 426-432 (2016).

150. Kumaki, J. *et al.* AFM snapshots of synthetic multifunctional pores with polyacetylene blockers: Pseudorotaxanes and template effects. *Angew. Chem. Int. Ed.* **44,** 6154-6157 (2005).

151. Talukdar, P., Bollot, G., Mareda, J., Sakai, N. & Matile, S. Synthetic ion channels with rigid-rod pi-stack architecture that open in response to charge-transfer complex formation. *J. Am. Chem. Soc.* **127,** 6528-6529 (2005).

152. Shen, Y. X. *et al.* Highly permeable artificial water channels that can self-assemble into two-dimensional arrays. *Proc. Natl. Acad. Sci. U S A* **112,** 9810-9815 (2015).

153. Liu, H. *et al.* Translocation of single-stranded DNA through single-walled carbon nanotubes. *Science* **327,** 64-67 (2010).

154. Tunuguntla, R. H., Allen, F. I., Kim, K., Belliveau, A. & Noy, A. Ultrafast proton transport in sub-1-nm diameter carbon nanotube porins. *Nat. Nanotechnol.* **11,** 639-644 (2016).

155. Lang, C. *et al.* Biomimetic transmembrane channels with high stability and transporting efficiency from helically folded macromolecules. *Angew. Chem. Int. Ed.* **55,** 9723-9727 (2016).

156. Bhosale, S. *et al.* Photoproduction of proton gradients with pi-stacked fluorophore scaffolds in lipid bilayers. *Science* **313,** 84-86 (2006).

157. Hall, A. R. *et al.* Hybrid pore formation by directed insertion of α-haemolysin into solid-state nanopores. *Nat. Nanotechnol.* **5,** 874-877 (2010).

158. Mantri, S., Sapra, K. T., Cheley, S., Sharp, T. H. & Bayley, H. An engineered dimeric protein pore that spans adjacent lipid bilayers. *Nat. Commun.* **4** (2013).

159. Burton, A. J., Thomson, A. R., Dawson, W. M., Brady, R. L. & Woolfson, D. N. Installing hydrolytic activity into a completely *de novo* protein framework. *Nat. Chem.* **8,** 837-844 (2016).

160. Costa, T. R. *et al.* Secretion systems in gram-negative bacteria: Structural and mechanistic insights. *Nat. Rev. Microbiol.* **13,** 343-359 (2015).

161. Franceschini, L., Soskine, M., Biesemans, A. & Maglia, G. A nanopore machine promotes the vectorial transport of DNA across membranes. *Nat. Commun.* **4,** 2415 (2013).

162. Watson, M. A. & Cockroft, S. L. Man-made molecular machines: Membrane bound. *Chem. Soc. Rev.* (2016).

163. Nivala, J., Marks, D. B. & Akeson, M. Unfoldase-mediated protein translocation through an α-hemolysin nanopore. *Nat. Biotechnol.* **31,** 247-250 (2013).

164. Noji, H., Yasuda, R., Yoshida, M. & Kinosita, K., Jr. Direct observation of the rotation of f1-atpase. *Nature* **386,** 299-302 (1997).

165. Bakelar, J., Buchanan, S. K. & Noinaj, N. The structure of the beta-barrel assembly machinery complex. *Science* **351,** 180-186 (2016).

166. Hendrickson, W. A. Atomic-level analysis of membrane-protein structure. *Nat. Struct. Mol. Biol.* **23,** 464-467 (2016).

167. Williams, J. K., Tietze, D., Lee, M., Wang, J. & Hong, M. Solid-state NMR investigation of the conformation, proton conduction, and hydration of the influenza b virus M2 transmembrane proton channel. *J. Am. Chem. Soc.* **138,** 8143-8155 (2016).

168. Hodel, A. W., Leung, C., Dudkina, N. V., Saibil, H. R. & Hoogenboom, B. W. Atomic force microscopy of membrane pore formation by cholesterol dependent cytolysins. *Curr. Opin. Struct. Biol.* **39,** 8-15 (2016).

169. Zhu, R. *et al.* Nanopharmacological force sensing to reveal allosteric coupling in transporter binding sites. *Angew. Chem. Int. Ed.* **55,** 1719-1722 (2016).

170. Krasilnikov, O. V., Rodrigues, C. G. & Bezrukov, S. M. Single polymer molecules in a protein nanopore in the limit of a strong polymer-pore attraction. *Phys. Rev. Lett.* **97,** 018301 (018301-018304) (2006).

171. Merzlyak, P. G., Capistrano, M. F. P., Valeva, A., Kasianowicz, J. J. & Krasilnikov, O. V. Conductance and ion selectivity of a mesoscopic protein nanopore probed with cysteine scanning mutagenesis. *Biophys. J.* **89,** 3059-3070 (2005).

172. Huang, S., Romero-Ruiz, M., Castell, O. K., Bayley, H. & Wallace, M. I. High-throughput optical sensing of nucleic acids in a nanopore array. *Nat. Nanotechnol.* **10,** 986-991 (2015).

173. Andersen, O. S. & Koeppe, R. E., 2nd Bilayer thickness and membrane protein function: An energetic perspective. *Annu. Rev. Biophys. Biomol. Struct.* **36,** 107-130 (2007).

174. Saliba, A. E., Vonkova, I. & Gavin, A. C. The systematic analysis of protein-lipid interactions comes of age. *Nat. Rev. Mol. Cell. Biol.* **16,** 753-761 (2015).

175. Miles, A. J. & Wallace, B. A. Circular dichroism spectroscopy of membrane proteins. *Chem. Soc. Rev.* **45,** 4859-4872 (2016).

176. Laganowsky, A. *et al.* Membrane proteins bind lipids selectively to modulate their structure and function. *Nature* **510,** 172-175 (2014).
177. Maffeo, C., Bhattacharya, S., Yoo, J., Wells, D. & Aksimentiev, A. Modeling and simulation of ion channels. *Chem. Rev.* **112,** 6250-6284 (2012).
178. Stansfeld, P. J. *et al.* Memprotmd: Automated insertion of membrane protein structures into explicit lipid membranes. *Structure* **23,** 1350-1361 (2015).
179. Blake, S., Capone, R., Mayer, M. & Yang, J. Chemically reactive derivatives of gramicidin A for developing ion channel-based nanoprobes. *Bioconj. Chem.* **19,** 1614-1624 (2008).

ADDITIONAL INFORMATION
Reprints and permission information is available online at www.nature.com/reprints. Correspondence and requests for materials should be addressed to SH.
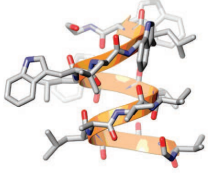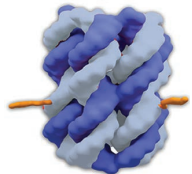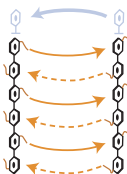
Box 1: The main structural features and functions of membrane nanopores.

Box 1

Nanoscale dimensions

Insertion

Hydrophobic belt

Hydrophillic inner channel wall

Hydrophobic membrane

Transport of water solutes

Molecular recognition

Nanomechanical opening
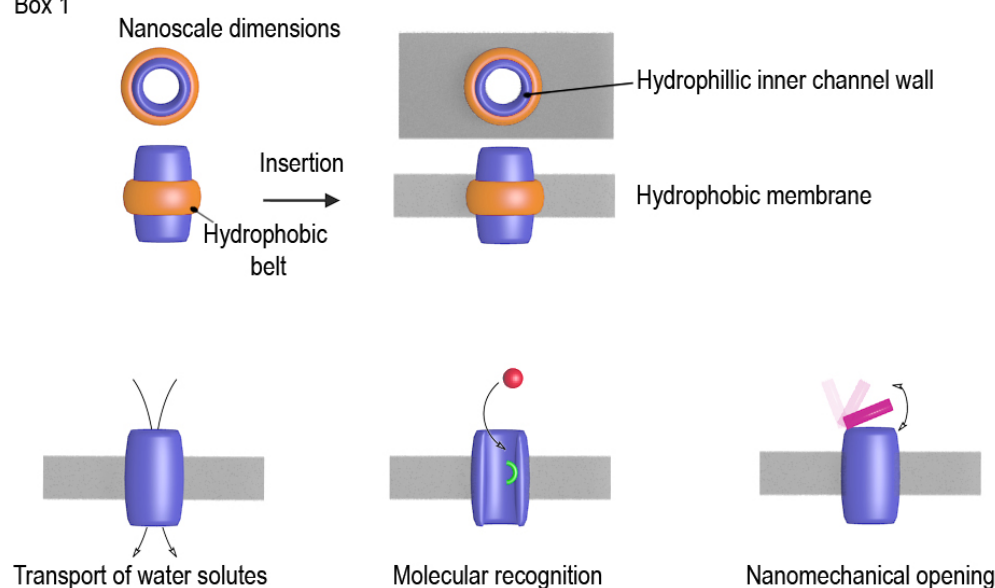
Box 2: The four classes of pores featuring the strengths and challenges of the building materials.

Protein	Peptide	DNA	Synthetic organic
+ Defined and stable scaffold	+ Many non-standard amino acids	+ Simple *de novo* design	+ Widest chemical repertoire
+ Simple engineering via amino acid changes	+ Non-protein structural folds	+ Dedicated design software	+ Flexible design
+ Targeted addition of synthetic components	+ Design from scratch	+ Structures >20 nm accessible	+ Compact sizes <5 nm
– *Re* or *de novo* design difficult	+ Fast insertion kinetics	– Limited chemical repertoire	– No unifying architectural principles
– Few defined pores wider >5 nm	– Simple architectures	– Structural fluctuations and electronic leakiness of walls	– Challenging structural analysis
	– Lumen <1.5 nm	– Slow insertion kinetics	– Inherent gating/closing of channel

**Box 3:** Analysis of membrane pores

Structural analysis: X-ray crystallography of isolated pores without membranes is the gold standard[58] even though cryo-EM is has gained resolution due to new detector technology[166]. NMR is suitable for smaller pores, also for membrane-inserted versions[167]. Atomic force microscopy only probes shape but is good for tracking structural dynamics of large membrane-inserted pores[168] and for measuring the forces in interactions between cargo and channel[169].

Membrane transport of electrolyte ions: Recording ionic flux through single channels provides high temporal and ionic resolution, and is compatible with pores within cellular and vesicle membranes, and planar or droplet-interface bilayers[40,87]. The current magnitude is a proxy for the dimensions of the inserted channel; its width is confirmed by size-dependent permeation of probe molecules and the blocking effect on current[125,170]. In a similar fashion, covalently attaching reagents can confirm the predicted position of residues in the channel[171]. For narrow or highly charged channels, ion selectivity measurements and optional placement of charged residues elucidates the ion-conducting path.

Membrane transport of fluorophores: Measurement of molecular flux can establish transport through wider pores, either via bulk measurements[85], or through fluorescence microscopic analysis of individual channels that are laterally mobile within supported bilayers[172] or corralled in arrays of small suspended membranes[38].

Interaction with membranes: Pore structure and function is modulated by properties of the lipid bilayers[173], and methods to assess the interaction include fluorescence microscopy and AFM, lipid pull-down assays, liposome microarray-based assays[174], circular dichroism[175], and ion-mobility mass spectrometry[176].

Simulations: Simulations provide a vital contribution to understand the structural dynamics of pores, transport properties, their interaction with bilayers, and energetic implications, mostly via molecular dynamics and also coarse-grained modeling[137,177,178].
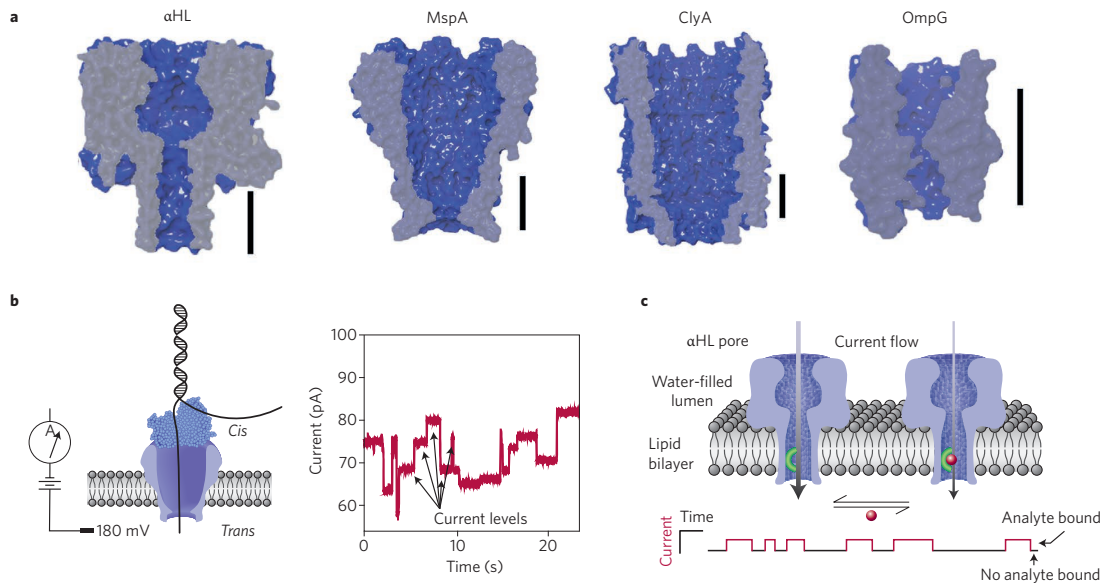
Figure 1 Protein pores and applications. a, X-ray structures of protein pores αHL, MspA, ClyA, and OmpG. The scale bar of 3 nm length is positioned where the pore spans the lipid bilayer. **b**, Sequencing with nanopores[4]. The left panel shows the membrane-inserted MpsA pore. A transmembrane potential pulls a negatively charged single-stranded DNA to the *trans* side and straighten the strand to facilitate base recognition by the reading head. A DNA polymerase motor protein (red) steps DNA and achieves controlled translocation to read the base translocation as current levels (left panel) which reflect not only the translocating base but also neighboring bases. **c**, Stochastic sensing to detect individual analyte molecules. In this approach, ionic current flowing through a single channel is monitoring as a function of time to detect binding of analyte molecule to an engineered binding site to produce current blockades. In equilibrium, the kinetic rate constant for binding $k_{on} = 1/\tau_{on}$ [A] where τ_{on} is the inter-event interval and [A] the analyte concentration, while the dissociation rate constant $k_{off} = 1/\tau_{off}$ whereby τ_{off} is the event duration or dwell time[71].
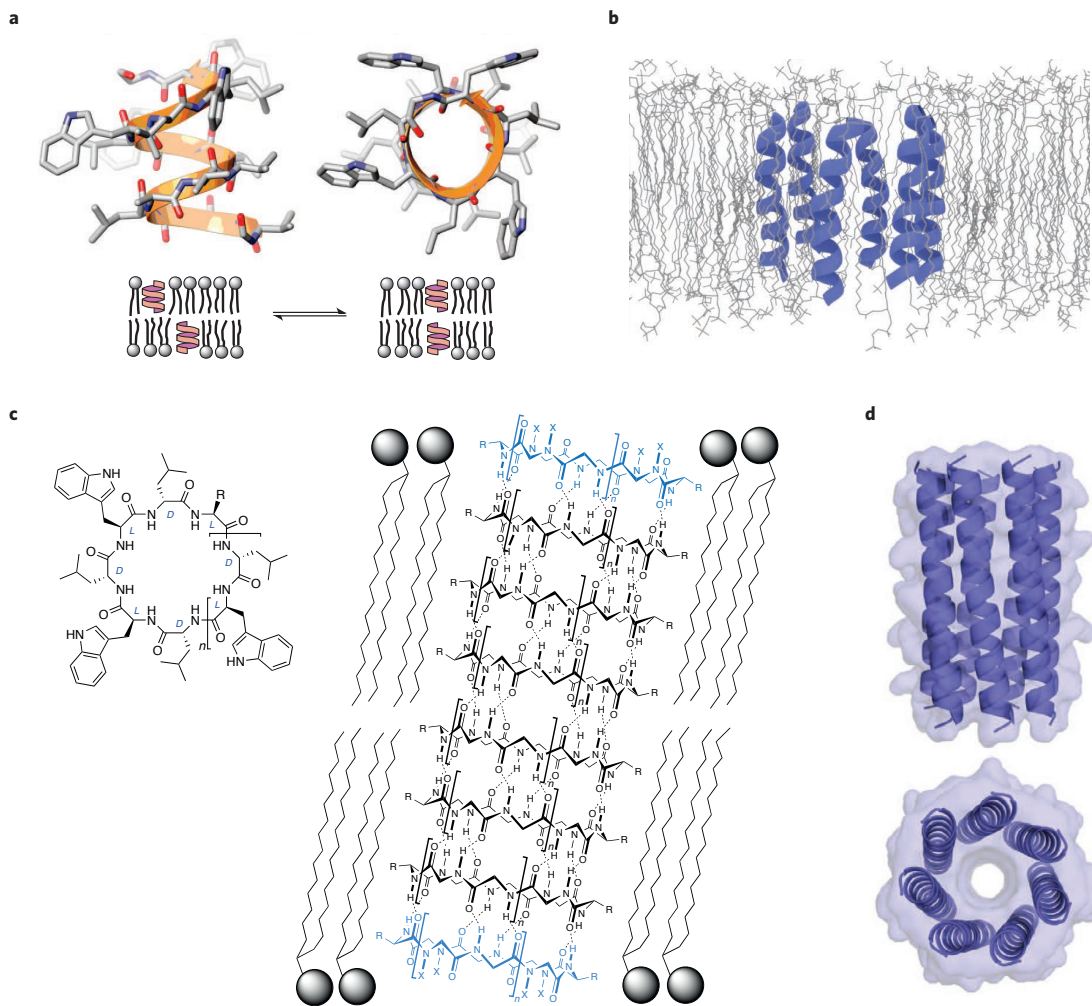
Figure 2 Peptide pores. **a**, Gramicidin forming a β-helix that spans one membrane leaflet but can transiently dimerize to form a membrane-spanning channel[179]. **b**, Model of α-helical alamethicin assembled into a six-stave barrel. **c**, A synthetic version composed of stacks of gramicidin-inspired peptide rings with an alternating sequence of D,L-amino acids[92]. **d**, Top and side view for the X-ray crystal structure of a *de novo* barrel with seven α-helices[104].
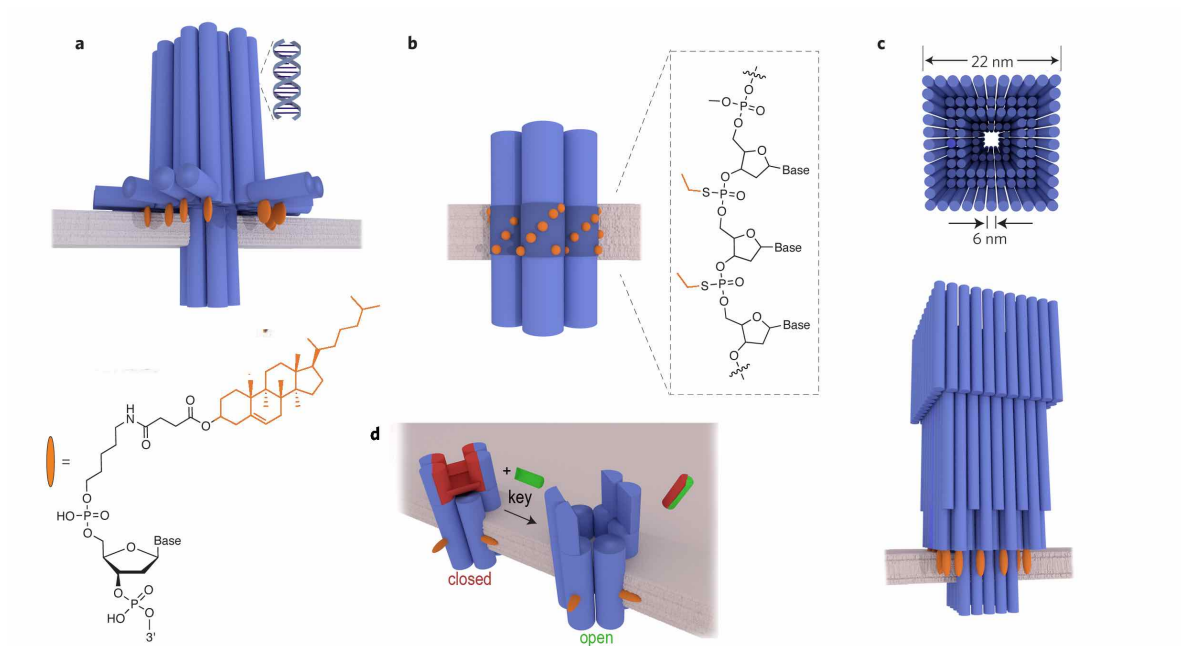
Figure 3 DNA nanopores composed of aligned duplexes. a, A pore assembled via the scaffold-and-staple approach. It features a large extramembrane cap region similar to protein pore αHL, and cholesterol lipid-anchors for membrane insertion[106]. **b**, A small six-duplex bundle composed solely of DNA oligonucleotides. A membrane-spanning hydrophobic belt is formed by charge-masked phosphate analogues ethyl phosphorothioate[107]. **c**, A DNA nanofunnel which spans the lipid bilayer with its cholesterol-modified narrow end[124]. **d**, A synthetic ligand-gated channel featuring a 'lock' DNA (red) in the closed nanopore state can be removed by hybridizing to 'key' DNA (green) to generate open-channel state[14].
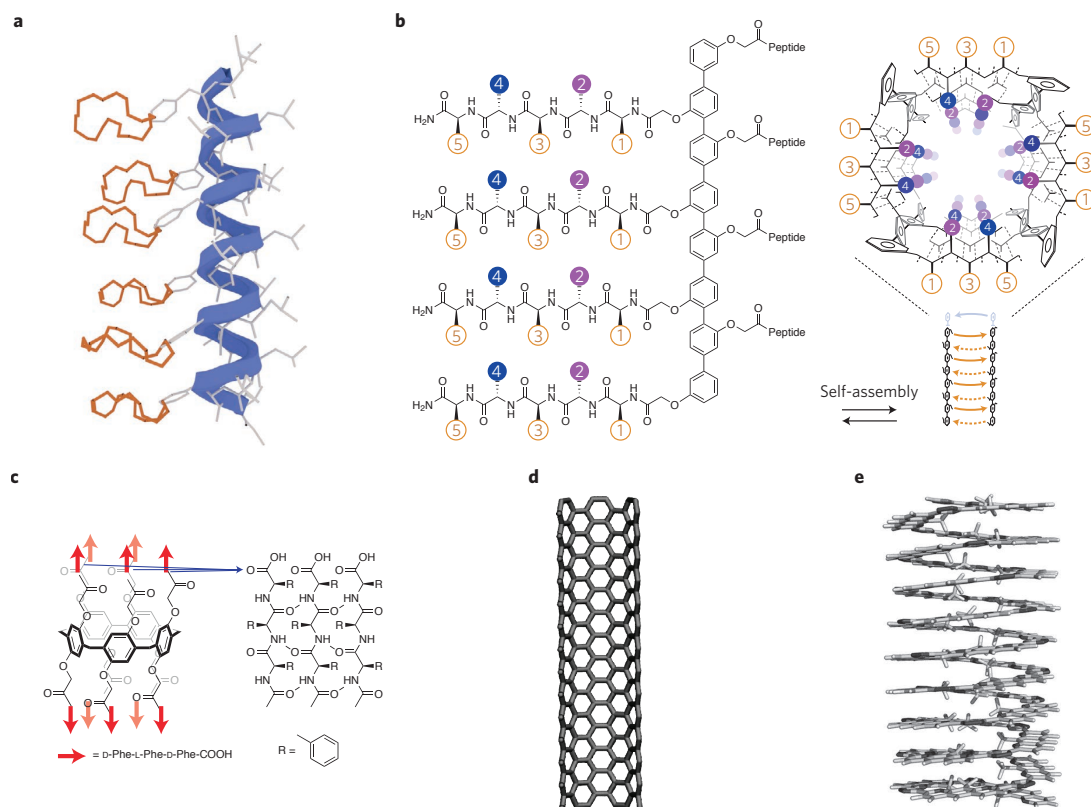
Figure 4 Organic synthetic nanopores. a, Crown ethers arranged in stack via a α-helical oligo-leucine scaffold[148]. **b**, Rigid-rod β-barrels with four octiphenyl rods that carry eight L-amino acid pentapeptides and interdigitate via H-bonding to assemble the pore[103]. **c**,Ppillar[5]arenes where each phenyl group of the five-membered circular arene carrying two short phenylalanine peptides of alternating D-L-D isomer sequence to form interstrand H-boding[152]. **d**, Single-wall carbon nanotubes[144]. **e**, Helically folded polymeric scaffolds based on oxadiazole-linked tricylic pyrido[3,2-g]quinolines and linear, membrane-interacting alkane extensions which are not shown in the model for reasons of visual clarity[155].